Electronic Structure of α,β-Unsaturated Ketones

Claude R. Jones and David R. Kearns*[1]

Contribution from the Department of Chemistry, University of California, Riverside, California 92502. *Received July 28, 1975*

Abstract: The high-resolution polarized singlet–triplet spectra of ketone I have been studied in detail. A partial analysis of the over 100 bands observed in the emission is suggested, and the polarization properties of various bands are accounted for in terms of Herzberg–Teller coupling of a $^3(\pi,\pi^*)$ state with the $^1(\pi,\pi^*)$ state and distortions in certain normal modes. The vibronic structure and polarization properties indicate there is little change in the geometry of the molecule upon excitation to its lowest $^3(\pi,\pi^*)$ state. This contrasts with certain theoretical calculations which predict that the molecule should be highly distorted in its lowest excited $^3(\pi,\pi^*)$ state. In order to account for the emission properties there is no need to invoke extensive mixing between the $^3(\pi,\pi^*)$ and $^3(n,\pi^*)$ states of this molecule. There is, however, extensive vibronic interaction between the $^3(\pi,\pi^*)$ state and upper vibrational levels of the $^3(n,\pi^*)$ state. Less complete studies were carried out on four related steroidal enones and entirely similar results were obtained with three of the compounds. It appears that the specific conclusions reached in the study of ketone I can be directly applied to other α,β-unsaturated ketones. The phosphorescence spectrum of 5-cholestenone was quite different from I and it is established that the lowest triplet state in this molecule is a $^3(n\pi^*)$, rather than a $^3(\pi,\pi^*)$ state. This result is important, since it provides a useful contrast to the other molecules which have a $^3(\pi,\pi^*)$ as the lowest excited state.

Simple α,β-unsaturated ketones display a remarkable range of photochemical reactions, including reduction, solvent addition, intramolecular cycloaddition, skeletal rearrangement, and other valence isomerizations. Because of this diversity, the photochemical properties of simple α,β-unsaturated ketones have been extensively studied.[2-22] In many studies there were attempts to deduce information about the nature of the reactive states indirectly from the nature of the products and the effect of various solvents and quenchers on the products, However, to understand why a particular reaction takes place, more information about the electronic structure of the molecule in its different excited states is usually required. For example, we would like to have information on the excited-state equilibrium geometries, the ordering of excited states, the difference between the ground- and excited-state charge distributions, and the extent to which the different excited states can be described in terms of pure (π,π^*) or (n,π^*), singlet or triplet states. This latter point is particularly important in the α,β-unsaturated ketones, where the (n,π^*) and (π,π^*) triplet states are nearly degenerate and could be extensively mixed by appropriate molecular distortions.[10]

In favorable circumstances, electronic spectroscopy can provide some of the required information and in previous papers we described the results of low-resolution investigations of a number of unsaturated ketones.[23] More recently we investigated the high-resolution singlet–triplet absorption spectra and the ODMR spectrum of single-crystal samples of the simple α,β-unsaturated ketone I.[24-26] While these studies provided information about the nature and ordering of low-lying excited states of this molecule, it was evident that a careful study of the phosphorescence emission spectrum could provide additional information, Furthermore, it remained to be demonstrated that the results obtained with ketone I could be extended to a discussion of the excited-state properties of other α,β-unsaturated ketones. In the present study we have carried out a detailed analysis of the polarized phosphorescence emission spectrum of single crystals of ketone I. For comparison, four other α,β-unsaturated ketones (II–V) were also studied and as we shall demonstrate, three of these compounds behave in a manner quite similar to I. One ketone (V), however, exhibited quite different properties and this is shown to be due to a change in the ordering of excited states from that found with ketones I–IV.

Experimental Section

9-Methyl-5(10)-octalin-1,6-dione (I in Figure 1) from Aldrich Chemical Co. was purified by triple vacuum sublimation. Its crystal structure has been determined and reported elsewhere.[24] Crystals were grown from diethyl ether, mounted, and their orientations determined from x-ray diffraction photographs. To avoid introducing artifacts into the optical polarization data from refractive index changes, spectra were only taken perpendicular to crystal faces. Since none of the natural crystal faces were favorably oriented with respect to the molecular axis, an experimental face of suitable orientation was cut and polished on each crystal. The oriented crystals were placed in a Dewar with their extinction or privileged directions oriented at 45° to the slits of the monochromator. A Polacoat quartz disk was used to select the desired direction of polarization before entering the monochromator.

Two different crystal orientations were used for the polarization experiments. In the first orientation an in-plane (95%) polarization along the C=C bond was compared with out-of-plane. In the second orientation both extinction directions were in the plane containing the four-atom enone chromophore with one direction (the long-axis direction) nearly along the C–C bond of the enone, but at an angle of 40° with the C=C bond and the other direction (the short-axis direction) was perpendicular to this (see Figure 2).

Testosterone (4-androsten-3-on-17-ol) (II), testosterone acetate (III) (Norell Chemical Co., Inc.), and 5-cholesten-7-on-3-β-ol acetate (V) were purified by crystallization from ethanol. Androstadienone (4,9(11)-androstadiene-3-one-17-methyl-17-ol) (IV) was purified by chromatography on alumina and crystals were grown from ethanol. Crystals of these ketones were immersed in liquid helium (4.2 K) and phosphorescence was excited by a 200-W high-pressure mercury lamp (366-nm line isolated by a Bausch and Lomb $f/3.5$ monochromator) and detected by a 0.3-m McPherson (Model 218) monochromator at 1.3-Å resolution. To obtain the phosphorescence excitation spectra the light from a 450-W xenon lamp was directed through the monochromator (1.3-Å resolution) and then to the sample. The resulting phosphorescence was detected through either a Corning 3-73 or 3-74 filter. An RCR 7265 photomultiplier was used for detection and the spectra were not corrected for its wavelength response (S-20).

Results and Discussion

A. 9-Methyl-5(10)-octalin-1,6-dione (I). (i) Authenticity of the Phosphorescence. The polarized spectra of the phosphorescence from single crystals of ketone I are shown in Figure 3. Even though a small amount of impurity could have given rise to all of the emission,[27] there are five reasons why we consider the emission to be authentic. First, the gap between the peaks of the 0–0 bands of the triplet absorption and emission (Figure 3) is about 30 cm^{-1}. Gaps of the 20–50 cm^{-1} are typically seen for authentic single-crystal phosphorescence from host molecules slightly perturbed by nearby crystal defects.[28,29] Second, the phosphorescence of I in a glassing solution (EPA) (no intermolecular energy transfer) is very similar to the emission profile seen in 4.2 K in the single crystal.

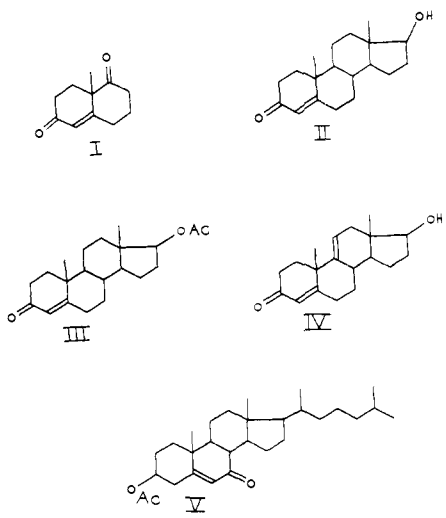

Figure 1, Molecular structures of the five α,β-unsaturated ketones studied.

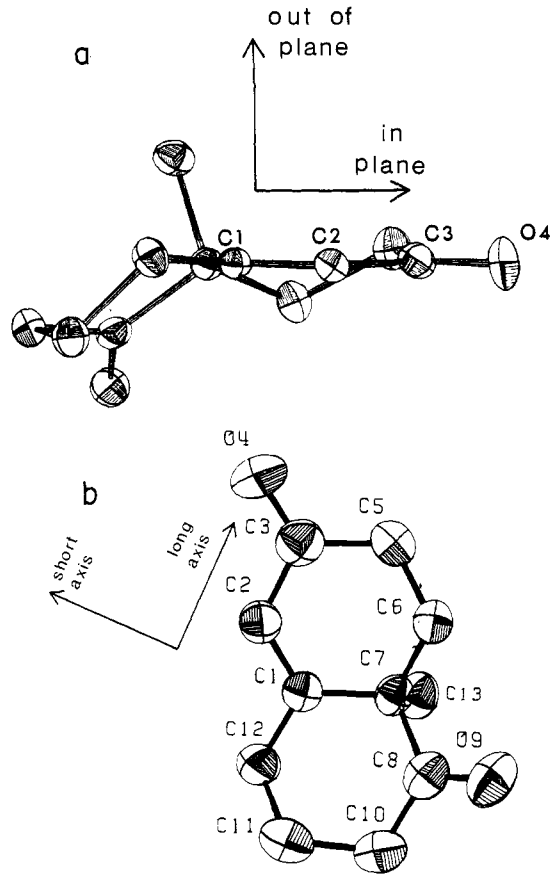

Figure 2, (a) Diagram showing the approximate orientation of ketone I used for the in-plane vs. out-of-plane polarization measurements. The in-plane extinction direction is nearly parallel to the $C_1{=}C_2$ double bond, being tipped just 5° out-of-plane. Since the two molecules per unit cell are related by a center of inversion, the polarization directions are the same for both. (b) Diagram showing the approximate orientation of ketone I used for measurement of the two in-plane polarization directions. The long-axis direction is exactly in-plane and makes an angle of 40° with the $C_1{=}C_2$ double bond.

Third, there is a close correspondence between the energy of the principal bands from the 0-0 band of the phosphorescence and infrared absorption bands. Fourth, the 4.2 K single-crystal emission has a lifetime of 20 ms, which compares favorably with the 30-ms lifetime seen in MTHF solutions of I. Fifth, *the 0-0 band of the phosphorescence (Figure 3) has the same polarization as the 0-0 band of the* $T_{\pi,\pi^*} \leftarrow S_0$ *absorption* (Figure 4), namely, nearly depolarized in-plane (short-axis favored slightly over the long-axis direction) and favoring the out-of-plane direction by 2/1 over the in-plane C=O direction. As we showed previously, these polarization properties are the same as the polarization properties of the 0-0 band of the $S_{n,\pi^*} \leftarrow S_0$ transition, which is predicted by spin-orbit coupling selection rules to be the source of intensity for the $T_{\pi,\pi^*} \leftarrow S_0$ transition.[24]

(ii) Vibrational Structure of the Phosphorescence. The vibrational bands observed in the phosphorescence (Figure 3) are of two distinct kinds, Bands 2, 3, 4, 15, 16, 17, 57, 58, 91, 93, and 94 have the same polarization as the 0-0 band, that is, out-of-plane polarization preferred over the in-plane and nearly depolarized in the in-plane long-axis short-axis comparison. Of these bands, band 57 (and its overtones, bands 91 and 94) and band 58 (and its overtone band 93) can be assigned as the C=C and C=O stretches, respectively, since corresponding bands in the infrared absorption are well known.

Most of the vibrational bands of the phosphorescence do not have the same polarization as the 0-0 band. Instead, they prefer the long-axis polarization in-plane and in the in-plane vs. out-of-plane comparison they are nearly depolarized. Because of these polarization properties, the majority of the bands in the spectrum are assigned as Herzberg-Teller (HT) bands, which are present because they bring in new sources of intensity stolen from a higher energy strongly allowed transition. The $^1(\pi,\pi^*)$ state is the likely source of this intensity because of its proximity, its high absorption strength, and the polarization properties observed in these vibronic bands. According to second-order perturbation theory there are two routes by which intensity in the $S_{\pi,\pi^*} \leftarrow S_0$ transition may be introduced into the $T_{\pi,\pi^*} \leftarrow S_0$ transition. Vibrational bands in the $S_{n,\pi^*} \leftarrow S_0$ transition can obtain intensity from the $S_{\pi,\pi^*} \leftarrow S_0$ transition by HT coupling and this intensity can be subsequently induced into the $T_{\pi,\pi^*} \leftarrow S_0$ transition by spin-orbit coupling. Alternatively, the $T_{n,\pi^*} \leftarrow S_0$ transition can obtain intensity from the $S_{\pi,\pi^*} \leftarrow S_0$ transition by spin-orbit coupling (i.e., the 0-0 band) and this intensity can be introduced into the $T_{\pi,\pi^*} \leftarrow S_0$ transition by HT coupling. Based on the relative energies of the states involved we conclude that intensity borrowing with the $^3(n,\pi^*)$ state as the intermediate is at least twice as important as the route involving the $^1(n,\pi^*)$ state.[24]

In molecules which have some symmetry, it is the asymmetric vibrations that are active in Herzberg-Teller coupling. For ketone I, however, all vibrations are symmetric, and the vibrations effective in HT coupling are asymmetric only in the sense that they destroy the local plane of symmetry of the enone chromophore. Some indication of the energy range in which strong HT bands should be expected can be obtained from data on acrolein and the methyl-substituted acroleins.[30,31] In these molecules, two out-of-plane bends are assigned in a range from 810 to 420 cm^{-1}, and the C=C and C-C torsions are assigned at 980 and 160 cm^{-1}, respectively. When the enone group is present in a ring system, these out-of-plane vibrations are coupled with some of the in-plane motions of the acroleins, such as the C=C—C and the C—C=O bends, which is assigned around 500 cm^{-1}. The prominent HT bands in the emission of ketone I are bands 19 and 24 at 547 and 674 cm^{-1}, and from the frequencies found for the acroleins we can at least say that these bands are in a frequency region consistent with out-of-plane motions that are expected to be involved in HT coupling.

The low-frequency bands in the phosphorescence (frequencies up to, say, 500 cm^{-1}) are in a range consistent with ring torsions and angle bends of the nonconjugated portions of the molecule. Ring torsions and ring puckering modes, for example, are usually around 100 cm^{-1}, but bands in the 200-500 cm^{-1} range most likely involve angle bends of the

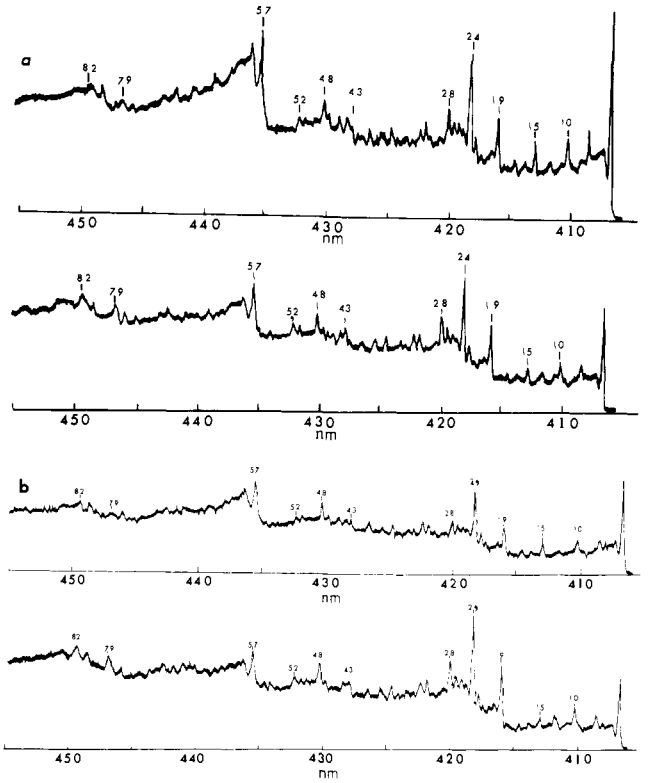

Figure 3. (a) Polarized phosphorescence spectrum of ketone I taken at 4.2 K. The upper spectrum is out-of-plane polarized and the lower spectrum is in-plane polarized. The more intense vibrational lines are 2, 3, 4, 5, 10, 13, 15, 16, 17, 19, 24, 28, 32, 48, 57, 58, 79, 82, 91, 93, and 94 at 36, 63-81, 108, 207, 301, 366, 423, 466, 547, 674, 777, 883, 1343, 1623, 1665, 2209, 2333, 3226, 3305, and 4818 cm^{-1} from the 0-0 band. (b) Polarized phosphorescence spectrum of ketone I taken at 4.2 K. The upper spectrum is short-axis polarized and the lower spectrum is long-axis polarized.

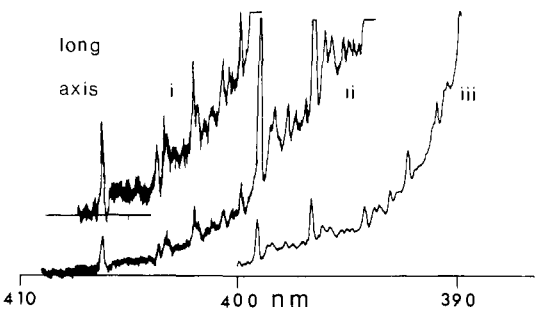

Figure 4. The $T_{n,\pi^*} \leftarrow S_0$ absorption of ketone I taken at 4.2 K. The gain for curve i is five times that used for curve ii, which in turn is five times that used for curve iii. The most prominent vibrational bands are 3, 6, 8, 9, 10, 14, 19, 23, and 27 at 146, 257, 338, 388, 438, 602, 749, 872, and 1029 cm^{-1}, respectively, from the 0-0 band.

carbon skeleton.[30-32] Both kinds of motion could distort the planarity of the enone chromophore, and thus, introduce HT intensity. Band 13, for example, and possibly bands 5 and 10 show some HT character, but the amount of HT activity in this region is not large. The indication, therefore, is that the bands in this region are not especially effective in disrupting the planarity of the enone chromophore and instead appear because the geometry, but not the local symmetry, of the $^3(\pi,\pi^*)$ state is changed from that of the ground state. Changes such as the relaxation of the C=C and C-C bonds of the enone could affect the ring twisting and angle bends of the nonconjugated part of the molecule and lead to the appearance of these bands in the phosphorescence.[33]

More specific assignments of the normal mode type have not been made, because relatively little is understood about the vibrational spectra of polycyclic enones in the regions of the infrared spectra that could be of use in assigning the rest of the phosphorescence bands.[34-36]

(iii) Geometry of the $^3(\pi,\pi^*)$ State of Ketone I. According to theoretical calculations the π,π^* states of acyclic conjugated enones are predicted to be highly distorted by twisting and the C=C,[37] and this has led some, including us,[23] to expect that the $^3(\pi,\pi^*)$ state of the cyclic enones might also be highly distorted. In a ring system, twisting about the C=C bond disrupts the planarity of the enone chromophore because this motion is coupled by the ring to other motions such as the twist about the C-C bond. The low-resolution spectra previously reported seemed to support this prediction, since the region of the 0-0 band was weak and followed by long progressions with Franck-Condon maxima far removed from the 0-0 band.[10] Following the report of these experiments, theoretical calculations were reported confirming that highly distorted π,π^* states for cyclic enones are consistent with a molecular orbital treatment of such states.[37] The high-resolution phosphorescence spectra given here, however, are not consistent with that earlier interpretation, since they show that the 0-0 band is quite strong and when allowance is made for the underlying continuum (discussed below), the 0-0 band is clearly the most intense feature of the phosphorescence. Thus, the excited-state distortion must be small. Furthermore, strong evidence for out-of-plane distortion is noticeably absent, since it was shown above that the prominent lines in the region of the out-of-plane bending of the chromophore obtain their intensity by HT coupling (rather than from a distortion along their normal coordinate), and are consistent with, at most, only a small amount of distortion in the out-of-plane direction. Excluding these HT lines, the most intense vibronic lines of the emission correspond to the stretches of the C=C and C=O bonds, but even the changes along these modes are quite modest relative to other ketones.[38] The polarization of the 0-0 band further supports the conclusion that the $^3(\pi,\pi^*)$ state is planar, or nearly so, since even small changes in the planarity of the enone chromophore would have strongly mixed in the $^3(\pi,\pi^*)$ state with the nearby $^3(n,\pi^*)$ state. Since the $T_{n,\pi^*} \leftarrow S_0$ transition is 100 times stronger than the $T_{\pi,\pi^*} \leftarrow S_0$ transition,[24] the polarization of the 0-0 band of the phosphorescence would have been strongly in-plane, long axis instead of mainly out-of-plane as is observed.

B. The Phosphorescence Spectra of Steroidal Enones. One reason for carrying out a detailed study of the relatively simple ketone I was that we expected it to have excited-state properties which were entirely similar to other steroidal enones which have been the subject of numerous spectral and photochemical studies. The results presented below serve to verify these expectations, and therefore permit the conclusions drawn from the study of ketone I to be used to understand the spectral properties of some of these steroidal enones.

(i) Testosterone Acetate (III). The low-temperature phosphorescence spectra of testosterone acetate single crystals and of a crystal of dihydrotestosterone acetate doped with testosterone acetate are shown in Figures 5a and 5b, A necessary consequence of the assignment of pure single-crystal phosphorescences as being due to slightly perturbed host molecules is that the same principal features should be seen in the phosphorescence spectrum regardless of whether the chromophore is a trap in its own host or a guest in a nonemitting host. Comparison of Figures 5a and 5b shows the principal features of these two emissions are indeed the same.

(ii) Testosterone (II) and Androstadienone (IV). The low-temperature phosphorescence spectra of testosterone and of androstadienone are shown in Figures 5c and 5d. These two enones differ from enones discussed previously in that both have an OH substituent. The OH group, however, is too far removed from the chromophore to exert an intramolecular

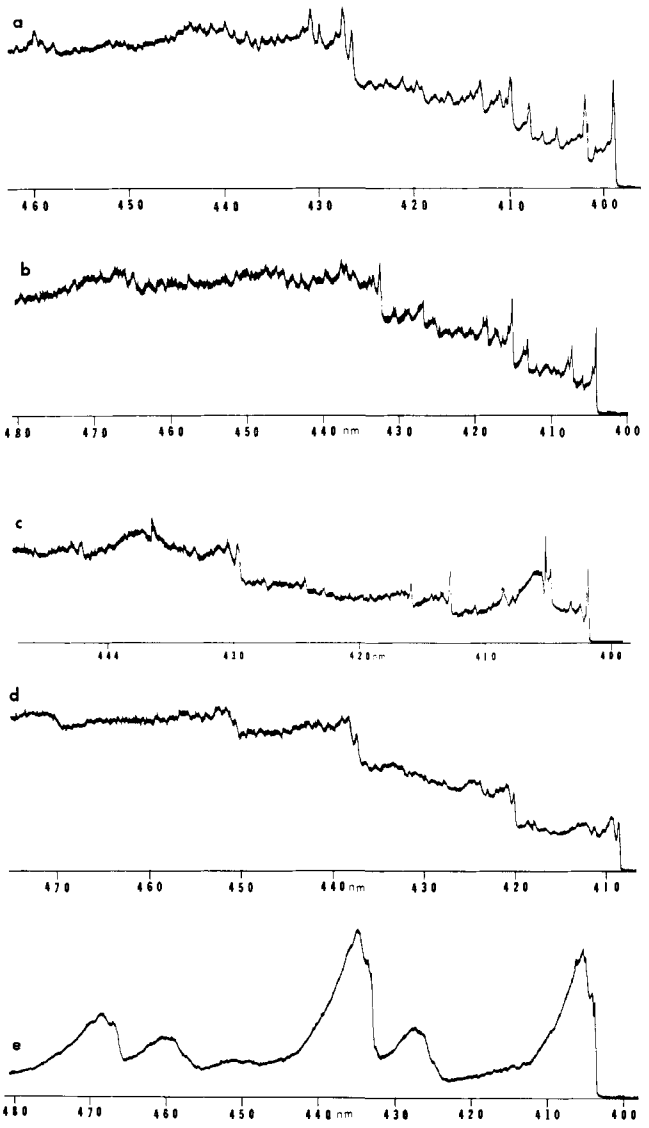

Figure 5. (a) The phosphorescence spectrum of testosterone acetate (III) single crystal taken at 4.2 K and a slit width of 50 μm. (b) The phosphorescence spectrum of testosterone acetate (III) in a crystal of dihydrotestosterone acetate taken at 4.2 K and a slit width of 50 μm. (c) Phosphorescence spectrum of testosterone (II) single crystal at 1.4 K. (d) Phosphorescence spectrum of androstadienone (IV) single crystal at 4.2 K. (e) Phosphorescence spectrum 5-cholesten-7-on-3-β-ol acetate (V) single crystal at 4.2 K.

effect on the molecular transition, and consequently the differences are attributed to intermolecular effects involving the OH group. If hydrogen bonding with the oxygen atom of the enone chromophore is the cause of the differences in the phosphorescence spectra, the effect of hydrogen bonding should be even more pronounced on the $S_{n,\pi^*} \leftarrow S_0$ transitions. This follows from the fact that the hydrogen bonding directly involves the nonbonding electrons of the enone oxygen, and these electrons are the ones most affected in transitions to the n,π^* states. In particular, the energies of the n,π^* states should be blue-shifted compared to non-hydrogen-bonding crystals, and in fact the splittings between the $^3(n,\pi^*)$ states and the $^3(\pi,\pi^*)$ states (which are less affected by hydrogen bonding)[39] of ketones II and IV are more than 300 cm^{-1} larger than the splittings usually seen.

(iii) 5-Cholesten-7-on-3-β-ol Acetate (V). The phosphorescence of ketone V is quite different from that of the ketones just discussed, as can be seen from Figure 5e. In this case the band structure of the phosphorescence is dominated by the carbonyl stretch rather than by vibrations involving the carbon skeleton,

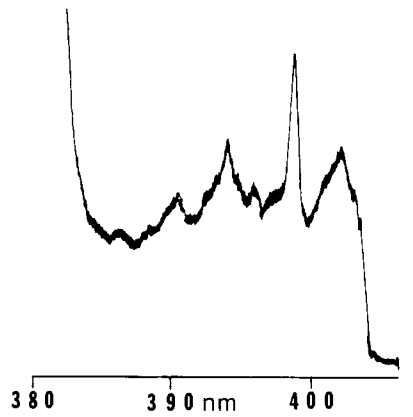

Figure 6. The $T_{n,\pi^*} \leftarrow S_0$ absorption of 5-cholesten-7-on-3β-ol acetate single crystal at 4.2 K.

and the lifetime, 2.5 ms, is much shorter than observed for the other ketones. Furthermore, the 0-0 band of the corresponding $T_{n,\pi^*} \leftarrow S_0$ absorption shown in Figure 6 overlaps the 0-0 band of the emission. All of these features together lead to the conclusion that this emission is from the $^3(n,\pi^*)$ state, rather than from the $^3(\pi,\pi^*)$ state, as was the case for the other ketones discussed.

Past assignments[23-26] of the lowest triplet state of most enones as a $^3(\pi,\pi^*)$ state were based on the fact that emission from these states lacked characteristics (vibrational structure, lifetime, etc.) which would be expected if the emission was from a $^3(n,\pi^*)$ state. The observation here of a clear case of $T_{n,\pi^*} \rightarrow S_0$ phosphorescence from an enone confirms these assignments.

C. Comparison of the Phosphorescence of Ketone I with Ketones II-IV. (i) Table I shows that the principal vibrational fundamentals in the $T_{n,\pi^*} \rightarrow S_0$ phosphorescence spectra of the four steroids correlate with the seven most prominent vibrational features of the spectrum of ketone I, which occur around 200, 540, 670, 780, 880, 1620, and 1666 cm^{-1}. In all five spectra, the later two vibrations are the main progression forming bands. Furthermore, the 0-0 band is a very prominent line in all of these spectra. The implication of these correlations is that the sources of intensity for the phosphorescence, as well as the geometries of the lowest triplet states of these steroidal enones, are similar to those of ketone I. The only pronounced difference among all these five systems is the 200-cm^{-1} region of testosterone, which is greatly enhanced in comparison with the same region in the other four systems. The band in this region of the emission of ketone I had polarization properties that suggest about equal contributions of allowed intensity appearing because of geometry changes and of HT intensity. Without oriented single-crystal polarized spectra of testosterone, it cannot be decided which of these sources is increased for testosterone.

(ii) Environmental Effects on the Zero Point Energies. This series of steroid spectra show a number of variations in the energies of the $T \rightarrow S$ transitions. Comparing the origin of the phosphorescence from a single crystal of testosterone acetate (Figure 5) with the origin of the phosphorescence observed from a single crystal of testosterone (Figure 5c), it can be seen that the 0-0 band moves from 404.2 to 401.9 nm, a blue shift of 139 cm^{-1}. Comparing testosterone acetate in its own crystal (Figure 5a) and testosterone acetate as a guest in dihydrotestosterone acetate crystals (Figure 5b) the 0-0 band of the $T_{\pi,\pi^*} \rightarrow S_0$ transition is blue-shifted 5.2 nm or 323 cm^{-1}. The $S_{n,\pi^*} \leftarrow S_0$ transition (Figures 7a and 7b) of testosterone acetate is red-shifted by 279 cm^{-1} in going from the single crystal to the mixed crystal. This indicates that the environment of the mixed crystal in the region of the enone chromophore is less polar than

Table I. Correlation of the Prominent Vibronic Bands of the Phosphorescence of Ketones I to IV

Ketone	Band	Energy, cm^{-1}
	Bands Near 200 cm^{-1}	
I	10	207
III	6	188
II	4 and 5	181 and 200
IV	4	214
	Bands Near 540 cm^{-1}	
I	19	547
III	11	540
II	11	536
IV	5	546
	Bands Near 670 cm^{-1}	
I	24	674
III	13	661
II	13	654
IV	7	676
	Bands Near 780 cm^{-1}	
I	28	777
III	14 and 15	765 and 788
II	16	777
IV		
	Bands Near 880 cm^{-1}	
I	32	883
III	17	851
II	18	834
IV	9 and 10	833 and 878
	Bands Near 1610 cm^{-1}	
I	57	1623
III	34	1624
II	22	1607
IV	18	1606
	Bands Near 1660 cm^{-1}	
I	58	1665
III	35	1672
II	23	1650
IV	19	1653

is the case in the single crystal. The shift of 279 cm^{-1} in the origin of the $S_{n,\pi^*} \leftarrow S_0$ transition is not surprising in view of the well-known solvent sensitivity of $n \rightarrow \pi^*$ transitions,[39] but the 323-cm^{-1} shift of the $T_{\pi,\pi^*} \rightarrow S_0$ transition is unexpectedly large, especially in light of the fact that the general appearance of the phosphorescence spectrum is unchanged. What these results show is that even the π orbitals of enones have a large interaction with their environment.

The strong interaction between the enone chromophore and the crystal environment is also manifested in the intensity distribution in the spectrum. Most of the intensity is in an underlying continuum which is probably due to phonon structure built on each of the sharp lines. The relative strength of the phonon sidebands can vary widely because it depends both on the strength of the guest–host coupling and on the amount of lattice distortion accompanying the electronic transition.[40] Thus, in contrast to ketone I, where sharp lines are very prominent in the phosphorescence, testosterone, androstadiene, and 5-cholestenone have a much greater contribution from the unresolved continuum. The OH groups of testosterone and androstadiene can provide an additional strong intermolecular coupling of the enone chromophore to the lattice. In the case of 5-cholesterone, the $T_{n,\pi^*} \rightarrow S_0$ transition directly involves the nonbonding orbital which is a major source of guest–host coupling. Consequently, the sharp lines in the phosphorescence are much less prominent relative to the phonon continuum.

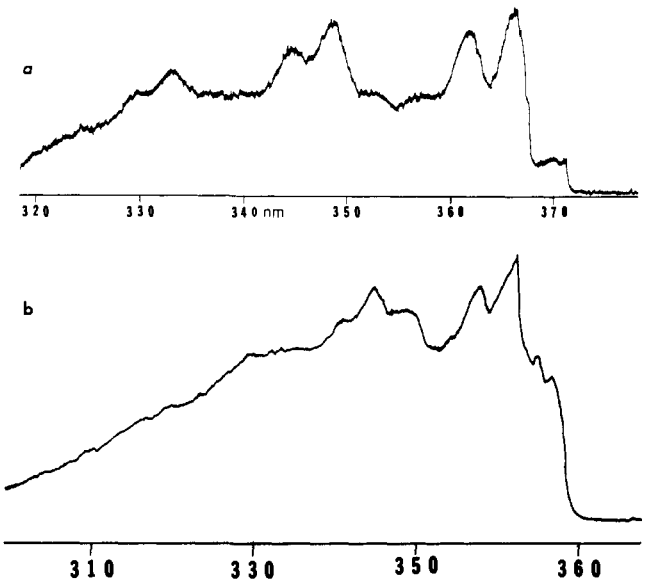

Figure 7. (a) The $S_{n,\pi^*} \leftarrow S_0$ absorption of testosterone acetate (III) in a single crystal of dihydrotestosterone acetate at 4.2 K. (b) The $S_{n,\pi^*} \leftarrow S_0$ absorption of testosterone acetate (III) single crystal at 4.2 K.

(iii) Photochemical Implications. The phosphorescence spectra of the four enones that have a $^3(\pi,\pi^*)$ state lowest show that the geometry of the $^3(\pi,\pi^*)$ state is nearly the same as the ground-state geometry and in particular that disruption of the planarity of the enone group is quite small. This is in sharp contrast to calculations and low-resolution phosphorescence studies, which indicated a highly nonplanar $^3(\pi,\pi^*)$ state. We now begin to understand why previous reports of highly distorted cyclic enone π,π^* states were wrong. With regard to the conclusions based on emission spectra,[10] it can be seen (Figure 3) that, while the 0–0 band is the most intense feature in the spectra, it accounts for only a small fraction of the total integrated intensity. Consequently, low-resolution spectra, such as those on which previous conclusions were based,[23] do not allow a proper appreciation of the intensity of the 0–0 band. The apparent long progression in these low-resolution spectra is also misleading because what appears to be a long progression of low-frequency (ca. 650 cm^{-1}) out-of-plane bending motions in the low resolution spectra is actually seen, in the high resolution spectra, to be two progressions. The first progression of the out-of-plane bending motions is actually very short, and the second progression does not involve out-of-plane bending at all, but instead is due to C=C and C=O bond stretches. This accounts for the conclusions derived from low-resolution emission spectra, but leaves unexplained the conclusions based on molecular orbital calculations. These calculations[37] strongly indicate that the π,π^* states are stabilized by twisting about the C=C bond. What these calculations also show, however, is that the π,π^* states are strongly destabilized by twisting about the C–C bond because of the increased double-bond character in this bond in the π,π^* states. In fused ring systems, these two twisting motions are strongly coupled together. Apparently, the increased double-bond character in the C–C overcomes the out-of-plane twisting tendencies of the C=C bond with the consequence that the enone chromophore remains essentially planar in the $^3(\pi,\pi^*)$ state.

The unsaturated enones exhibit a number of photoisomerizations which proceed from the triplet state. Since these reactions necessarily involve large changes in geometry, we had anticipated that the geometry of the emitting state would be intermediate between the geometries of the ground states of the starting material and the products, but this is clearly not

the case. One possibility is that the photochemical products are formed in a radiationless transition from the $^3(\pi,\pi^*)$ state with a planar enone chromophore to the ground state of the products with a very different geometry. This, however, seems unlikely for two reasons. First, the Franck–Condon factors for such a radiationless transition would be very unfavorable. Second, chemical evidence suggests that the photochemistry proceeds on a nanosecond time scale and if this were occurring from the zeroth vibrational level of the lowest triplet, then the phosphorescence would have a very short lifetime and a very low quantum yield; in fact, it would be unobservable. The more likely possibility is that geometry changes leading to products occur along pathways that are inaccessible at 77 or 4 K, where strong phosphorescence is observed, but which are thermally activated at room temperature, where the photochemistry is observed.

Acknowledgment. The support of the U.S. Public Health Service (GM 10449) is gratefully acknowledged. We also wish to thank Professor Kurt Schaffner for many helpful discussions.

References and Notes

(1) Present address: Department of Chemistry, University of California, San Diego, La Jolla, California 92037.
(2) (a) K. Schaffner, *Pure Appl. Chem.* **33**, 329 (1973); (b) *ibid.*, **16**, 75 (1968).
(3) O. Jeger and K. Schaffner, *Pure Appl. Chem.*, **21**, 247 (1970).
(4) W. A. Noyes, Jr., G. S. Hammond, J. N. Pitts. Jr., and K. Schaffner, *Adv. Photochem.* **4**, 81 (1966).
(5) H. E. Zimmerman, *Science*, **153**, 837 (1966).
(6) H. E. Zimmerman and R. D. Little, *J. Chem. Soc., Chem. Commun.*, 689 (1972).
(7) S. Domb and K. Schaffner, *Helv. Chim. Acta*, **53**, 677 (1970).
(8) S. Domb, G. Bozzato, J. A. Saboz, and K. Schaffner, *Helv. Chim. Acta*, **52**, 2436 (1969).
(9) D. Bellus, D. R. Kearns, and K. Schaffner, *Helv. Chim. Acta*, **52**, 971 (1969).
(10) G. Marsh, D. R. Kearns, and K. Schaffner, *Helv. Chim. Acta*, **51**, 1890 (1968).
(11) P. Keller, F. G. Eggart, H. Wehrili, K. Schaffner, and O. Jeger, *Helv. Chim. Acta*, **50**, 2259 (1967).
(12) H. E. Zimmerman and N. Lewin, *J. Am. Chem. Soc.*, **91**, 879 (1969).
(13) H. E. Zimmerman and D. R. Amick, *J. Am. Chem. Soc.*, **95**, 3977 (1973).
(14) R. L. Cargill, A. B. Sears, J. Boehm, and M. R. Willcott, *J. Am. Chem. Soc.*, **95**, 4346 (1973).
(15) S. Wolff, W. L. Schreiber, A. B. Smith, III, and W. C. Agosta, *J. Am. Chem. Soc.*, **94**, 7797 (1972).
(16) W. C. Agosta and A. B. Smith, III, *J. Am. Chem. Soc.*, **93**, 5513 (1971).
(17) L. E. Friedrich and G. B. Schuster, *J. Am. Chem. Soc.*, **94**, 1193 (1972).
(18) P. J. Wagner and D. J. Bucheck, *J. Am. Chem. Soc.*, **91**, 5091 (1969).
(19) R. A. Schneider and J. Meinwald, *J. Am. Chem. Soc.*, **89**, 2023 (1967).
(20) P. de Mayo, *Acc. Chem. Res.*, **4**, 41 (1971).
(21) D. J. Patel and D. I. Schuster, *J. Am. Chem. Soc.*, **90**, 5137 (1968).
(22) W. G. Dauben, M. S. Kellogg, J. I. Seeman, and W. A. Spitzer, *J. Am. Chem. Soc.*, **92**, 1786 (1970).
(23) G. Marsh, D. R. Kearns, and K. Schaffner, *J. Am. Chem. Soc.*, **93**, 3129 (1971).
(24) C. R. Jones, D. R. Kearns, and R. M. Wing, *J. Chem. Phys.*, **58**, 1370 (1973).
(25) C. R. Jones, F. Pappano, A. H. Maki, and D. R. Kearns, *Chem. Phys. Lett.*, **13**, 521 (1972).
(26) C. R. Jones, A. H. Maki, and D. R. Kearns, *J. Chem. Phys.*, **59**, 873 (1973).
(27) R. M. Hochstrasser, *J. Chem. Phys.*, **39**, 3153 (1963).
(28) A. Nakahara, M. Koyanagi, and Y. Kanda, *J. Chem. Phys.*, **50**, 552 (1969).
(29) S. Dym, R. M. Hochstrasser, and M. Schafer, *J. Chem. Phys.*, **48**, 646 (1968).
(30) J. C. D. Brand and D. G. Williamson, *Discuss. Faraday Soc.*, **35**, 184 (1963).
(31) R. R. Birge, W. C. Pringle, and P. A. Leermakers, *J. Am. Chem. Soc.*, **93**, 6715 (1971).
(32) J. Laane, private communication.
(33) P. Petelenz and B. Petelenz, *J. Chem. Phys.*, **62**, 3482 (1975).
(34) R. N. Jones, F. Herling, and E. Katzenellenbogen, *J. Am. Chem. Soc.*, **77**, 651 (1955).
(35) R. N. Jones, B. Nolin, and G. Roberts, *J. Am. Chem. Soc.*, **77**, 6331 (1955).
(36) S. Weinmann and J. Weinmann, *C. R. Acad. Sci.*, **256**, 2578 (1963).
(37) A. Devaquet, *J. Am. Chem. Soc.*, **94**, 3160 (1972).
(38) W. A. Case and D. R. Kearns, *J. Chem. Phys.*, **52**, 2175 (1970).
(39) S. Iwata and K. Morokuma, *J. Am. Chem. Soc.*, **97**, 966 (1975).
(40) R. Hochstrasser and P. Prased, *J. Chem. Phys.*, **56**, 2814 (1972).

An ab Initio Investigation of $(Formamide)_n$ and Formamide–$(H_2O)_n$ Systems. Tentative Models for the Liquid State and Dilute Aqueous Solution

J. F. Hinton* and R. D. Harpool

Contribution from the Department of Chemistry, University of Arkansas, Fayetteville, Arkansas 72701. *Received February 20, 1976*

Abstract: Ab initio molecular orbital calculations (STO-3G) have been made on large systems in an attempt to simulate the hydrogen bonding of formamide in the liquid state and in dilute aqueous solutions. Although the relationship between the model systems (formamide + $(H_2O)_4$ molecules representing an aqueous-formamide solution and $(formamide)_5$ molecules representing the liquid state of pure formamide) and the liquid state is crude, the calculations appear to be in reasonable agreement with experimental results and provide insight into the bonding and structure of these solutions not obtainable by experiment.

The importance of hydrogen bonding in biological systems has led to a number of experimental and theoretical studies of model compounds capable of participating in the type of hydrogen bonding found in these systems. Amides have been chosen as model systems because they are the simplest molecules that exhibit peptide bonding. Information gained concerning hydrogen bonding in amide and aqueous-amide solutions, therefore, should give insight into the hydrogen-bonding mechanisms found in the more complex biological systems. Amides have also been used extensively as solvents and as solvent components in mixed solvent systems; however, the bonding and structure of these amide and aqueous-amide solutions are still not well understood.[1]

The interpretation of experimental results appears to be somewhat inconsistent with respect to the relative strength of amide and amide-water hydrogen bonds.[2-5] Nuclear magnetic resonance studies in our laboratory of amide and aqueous-amide solutions over the complete mole fraction range did not permit the determination of all of the hydrogen-bond sites on the amides or their relative importance in solution.[6-8]